Splenic erythrophagocytosis is regulated by ALX/FPR2 signaling

Haley Asplund, Hector H. Dreyer, Jing-Juan Zheng, Richa Singhal, Jason L. Hellmann and Brian E. Sansbury

Center for Cardiometabolic Science, Christina Lee Brown Envirome Institute, Division of Environmental Medicine, Department of Medicine, University of Louisville, Louisville, KY, USA

Correspondence: B.E. Sansbury
Brian.Sansbury@Louisville.edu

Received: April 11, 2025.
Accepted: August 29, 2025.
Early view: September 11, 2025.

https://doi.org/10.3324/haematol.2025.288007

Abstract

Maintaining a healthy pool of circulating red blood cells (RBC) is essential for adequate perfusion, as even minor changes in the population can impair oxygen delivery, resulting in serious health complications including tissue ischemia and organ dysfunction. This responsibility largely falls to specialized macrophages in the spleen, known as red pulp macrophages, which efficiently take up and recycle damaged RBC. However, questions remain regarding how these macrophages are acutely activated to accommodate increased demand. Proresolving lipid mediators stimulate macrophage phagocytosis and efferocytosis but their role in erythrophagocytosis has only recently been described. To investigate the role of lipid mediators in red pulp macrophage function, we targeted the ALX/FPR2 signaling pathway, as this receptor binds multiple lipid mediator ligands eliciting potent macrophage responses. We found that mice with *Fpr2* deletion exhibited disrupted erythrocyte homeostasis resulting in an aged RBC pool, decreased markers of splenic RBC turnover, and altered splenic macrophage phenotype characterized by changes in heme metabolism. Upon activation of on-demand erythrophagocytosis, production of the ALX/FPR2 ligand, lipoxin A_4 (LXA_4), was induced in the spleen while receptor-deficient animals were unable to efficiently clear damaged RBC, a defect that was conserved in mice with myeloid-specific *FPR2* deletion. Similarly, mice lacking the LXA_4 biosynthetic enzyme displayed defective erythrophagocytosis that was rescued with LXA_4 administration. These results indicate that the ALX/FPR2 signaling axis is necessary for maintenance of RBC homeostasis and that LXA_4 activation is a critical aspect of the red pulp macrophage response to acute erythroid stress.

Introduction

Red blood cells (RBC) are the most abundant cell type in the body and are traditionally appreciated for their role in respiration and gas exchange. Recently, RBC have garnered new attention for their immunomodulatory effects, which are primarily achieved via their interaction with resident macrophages in the spleen – known as red pulp macrophages (RPM).[1,2] As erythrocytes enter the spleen, RPM probe the cells for signs of mechanical and oxidative damage, as well as inflammatory stimuli bound to cell surface receptors (e.g., foreign pathogens, endogenous chemokines).[1] Once recognized, RPM prune damaged portions of erythrocyte membranes or phagocytose the cell entirely, efficiently processing and recycling the cellular cargo.[3] In a healthy human this process, termed erythrophagocytosis, accounts for the daily turnover of roughly 150-200 billion RBC.[3,4] Consequently, defects in the system can impact physiological iron recycling and induce wide-ranging effects on health including anemia, impaired host defenses, and even sepsis.[2]

While much is known about the process of erythrophagocytosis, critical questions remain regarding the fundamental regulatory mechanisms that govern its activation and function. Of particular interest is the RPM response to increased erythrophagocytic demand as may be encountered during acute hemolytic reactions induced by transfusions,[5,6] infection,[7] autoimmunity,[8] or genetic disorders.[9] Addressing these gaps in knowledge presents a significant opportunity for developing therapeutics for conditions such as transfusion-related immunomodulation and sickle cell disease. Lipid mediators derived from the enzymatic conversion of polyunsaturated fatty acids (PUFA) are a newly appreciated class of autacoid signaling molecules that have dramatic impacts on immune cells, including macrophages.[10,11] In particular, specialized proresolving lipid mediators (SPM) bind

G protein-coupled receptors, such as ALX/FPR2, on macrophages enhancing migration, phagocytosis, and efferocytosis while limiting proinflammatory cytokine production, thereby promoting the active resolution of inflammation.[12-16] SPM activation of ALX/FPR2 is linked to improvements in numerous inflammatory conditions (e.g., atherosclerosis, heart failure, diabetes[17,18]) and, as we have demonstrated, plays a vital role in hastening tissue repair processes after injury.[19-21]

While the role of the SPM-ALX/FPR2 signaling axis in promoting macrophage clearance of pathogens, debris, and apoptotic cells is well documented, its impact on RBC disposal has only recently been demonstrated.[22,23] These studies establish the foundation that SPM, including ligands of ALX/FPR2, are involved in macrophage-mediated RBC clearance; however, it remains incompletely understood whether ALX/FPR2 signaling contributes to basal erythroid homeostasis and what role its activation plays during cases of acutely increased erythrophagocytosis.

Here, we present evidence that the ALX/FPR2 receptor is required for optimal homeostatic RBC turnover and is critical in facilitating splenic macrophage-mediated erythrophagocytosis. These results demonstrate the importance of the ALX/FPR2 signaling axis in coordinating RPM function and further illustrate the potent immunomodulatory ability of SPM to govern fundamental physiological processes.

Methods

Detailed methods are available in the accompanying *Online Supplementary Material.*

Animals and reagents

Male C57BL/6J (#00664), *Spic*-EGFP (#025673), and *Alox15*$^{-/-}$ (#002778) mice were from Jackson Laboratories (Bar Harbor, ME, USA). *Fpr2*$^{-/-}$ and wild-type (C57BL/6Ntac) mice were provided by Idorsia Pharmaceuticals and bred on-site. Mice with myeloid-specific deletion of h*FPR2* were generated as previously described[21] by crossing humanized *ALX/FPR2-GFP* floxed mice (provided by Idorsia) with commercially available LysM-Cre mice (Jackson; #004781). All procedures were performed in accordance with ethical regulations and pre-approved by the University of Louisville Institutional Animal Care and Use Committee. Lipoxin A_4 (LXA_4) was purchased from Cayman Chemical (Ann Arbor, MI, USA). Antibodies used for flow cytometry were purchased from BioLegend (San Diego, CA, USA).

In vivo red blood cell turnover

Biotin was administered intravenously and tail blood was sampled serially. RBC biotin expression was determined by flow cytometry.

RNA sequencing

RNA was isolated from mouse spleen and F4/80$^+$ splenocytes and subjected to poly-A RNA sequencing. An Abclonal second strand synthesis module kit was utilized for library construction. Paired-end sequencing was performed on an Illumina NovaSeq X Plus using the 25B Flow Cell. RNA-sequencing data have been deposited in the NCBI GEO database with accession numbers GSE292685 and GSE292686.

In vivo splenic red blood cell uptake

RBC from donor mice were oxidized with 0.2 mM copper(II) sulfate ($CuSO_4$) and 5 mM L-ascorbic acid or incubated with 10 μg/mL CD47 antibody (Bio X Cell) or 10 μg/mL mouse IgG isotype control (Bio X Cell, BE0083). RBC ($2x10^8$ cells) were labeled with carboxyfluorescein succinimidyl ester (CFSE) and administered intravenously to mice. After 1 hour, spleens were collected.

Ex vivo splenocyte red blood cell uptake

Single-cell suspensions were generated from spleens using a 70 μM cell strainer with RPMI 1640 supplemented with 10% fetal bovine serum (FBS) using the plunger from a 5 mL syringe. The suspension was centrifuged and RBC lysis was performed. The suspension was centrifuged and resuspended in RPMI 1640 with 10% FBS and 2 mM EDTA. Oxidized, CFSE-labeled RBC were added (1:10; splenocyte:RBC ratio) and incubated for 1 hour at 37°C, with gentle agitation every 15 minutes. Tubes were placed on ice to stop phagocytosis and centrifuged, and then RBC lysis was performed. Samples were centrifuged and resuspended in cell staining buffer prior to antibody staining for flow cytometry analysis.

Targeted lipidomics

Spleens were placed in methanol containing commercially available deuterium-labeled synthetic standards (PGE_2-d4, 15d-PGJ_2-d4, LTB_4-d4, LXA_4-d5, 11,12-EET-d11, 15-HETE-d8, 5-HETE-d8, RvE1-d4, RvD2-d5, RvD3-d5, MaR1-d5, and MaR2-d5) then stored at -80°C prior to being minced. Samples were acidified and added to C18 SPE columns. Neutral lipids were removed from the column using *n*-hexanes while lipid mediators were eluted with methyl formate. Using N_2 gas, solvent was evaporated and samples resuspended in methanol:water (50:50, v/v). Samples were analyzed using a Shimadzu liquid chromatography system (LC 20-AD with an SIL-20AC autoinjector) coupled to a QTrap5500 mass spectrometer operated in negative polarity mode. Lipid mediator identification was based on the following criteria: chromatographic peak retention time matching that of synthetic standards run in parallel (± 0.1 min); signal:noise ratio >5; and an on-column calculated concentration above the lower limit of quantification for each mediator. Absolute quantification was achieved by comparing samples to a 12-point standard curve of synthetic standards run in parallel. SCIEX OS (v.2.0.1) software was used for peak identification and quantification.

Statistical analysis

Data are presented as mean ± standard error of the mean. Statistical differences between groups were determined by performing a two-tailed, unpaired Student *t* test or two-way analysis of variance (ANOVA) using GraphPad Prism version 10. Statistical significance is denoted as: **P*<0.05, ***P*<0.01, ****P*<0.001, *****P*<0.0001. *P* values *>0.05* are considered not statistically significant (NS). Schematics used in figures were created using BioRender.

Results

Erythroid homeostasis is perturbed in mice lacking the ALX/FPR2 receptor

Previous studies have suggested a link between pro-resolving lipid mediator ligands of ALX/FPR2 and senescent RBC uptake and disposal.[22,23] To better understand the role of signaling via ALX/FPR2 in basal RBC homeostasis, we questioned whether deletion of the receptor would impact erythrocyte turnover. Using an *in vivo* two-step labeling approach[24] wild-type (WT) mice and mice lacking the ALX/FPR2 receptor (*Fpr2*$^{-/-}$) were first given a high dose of biotin followed 5 days later by a second lower dose. This method allows for the relative age of circulating RBC to be distinguished based on biotin signaling intensity. Over the course of 1 week following the second biotin administration, we found that the abundance of Biotin^{Hi} cells remained elevated while there was a reduced appearance of Biotin^{Neg} cells in *Fpr2*$^{-/-}$ mice compared with WT mice (Figure 1A, B), indicating that the rate of RBC turnover was significantly decreased in *Fpr2*$^{-/-}$ mice. To further characterize the state of the circulating erythroid pool in *Fpr2*$^{-/-}$ mice, we investigated the expression of CD47, an important marker of 'self' which is expressed highly on erythroblasts, preventing their premature uptake and clearance, and progressively

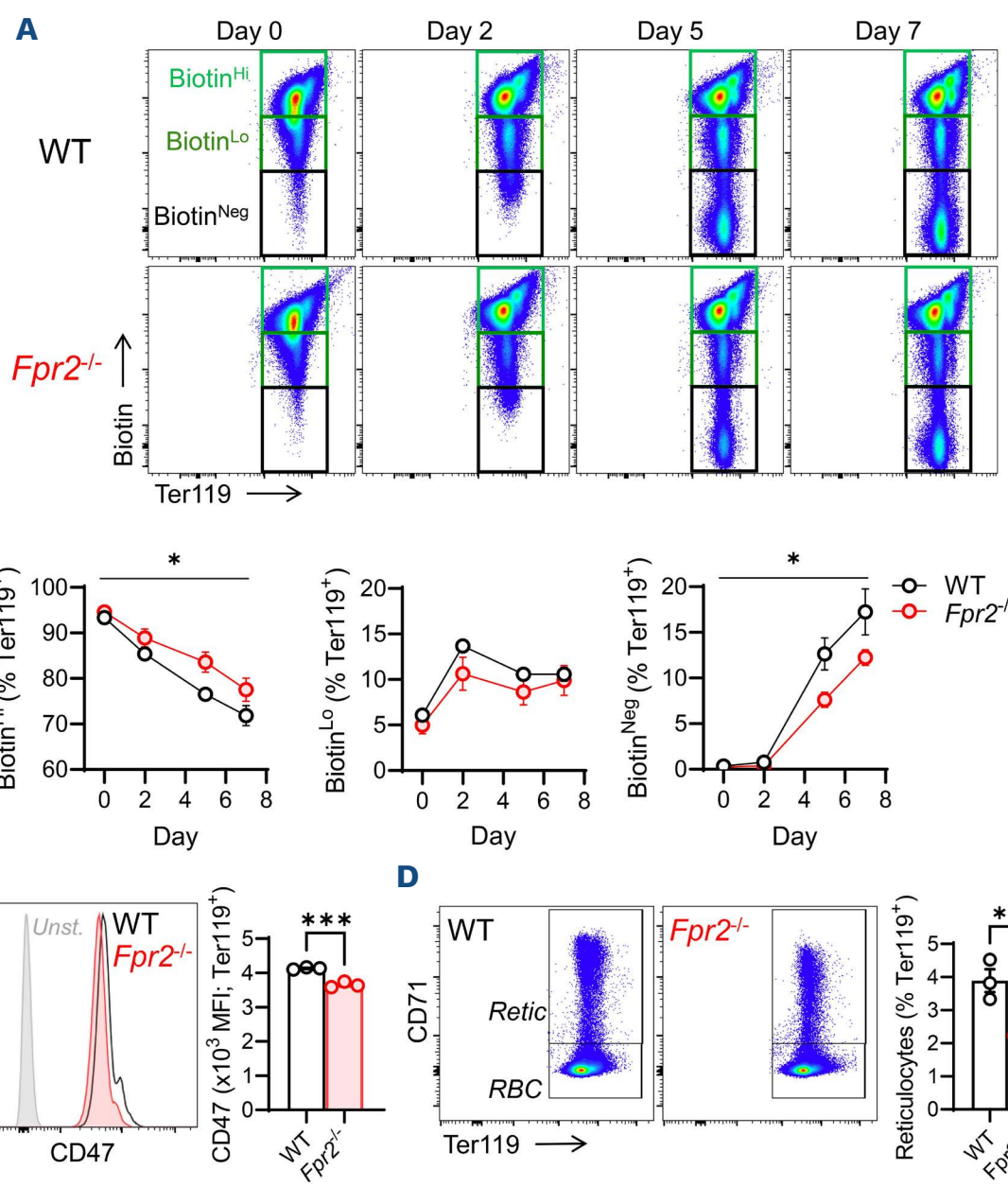

Figure 1. Deletion of the ALX/FPR2 receptor disrupts red blood cell turnover. The basal rate of red blood cell (RBC) turnover in wild-type (WT) mice and mice lacking the ALX/FPR2 receptor (*Fpr2*$^{-/-}$) was determined by a two-step biotinylation assay. (A) Representative flow cytometry dot plots are shown. Circulating RBC (Ter119^{+}) were gated based on biotin positivity. (B) Quantification of each RBC population is shown over time. (C) Representative flow cytometry histogram and quantification of CD47 expression on circulating RBC. (D) Representative flow cytometry dot plots and quantification of circulating reticulocytes (Retic; CD71^{+}Ter119^{+}). Data are mean ± standard error of mean. **P*<0.05, ***P*<0.01, ****P*<0.001 as determined by two-way analysis of variance or an unpaired Student *t* test.

decreases with age and stress on circulating RBC.[25] We found lower levels of CD47 in *Fpr2*$^{-/-}$ mice (Figure 1C), indicating an aged RBC population. Additionally, we examined the abundance of circulating reticulocytes as a measure of erythroid cells newly released into the circulation and found that these too were decreased in *Fpr2*$^{-/-}$ mice (Figure 1D). To determine whether decreased circulating reticulocytes were a result of changes in erythropoiesis, we analyzed erythroid precursor populations in the bone marrow of WT and *Fpr2*$^{-/-}$ mice. Interestingly, we found that the number of total erythroblasts and reticulocytes was not different between strains but the distribution of subpopulations was altered, suggesting potential dysregulation in the erythroblast maturation process and release of reticulocytes into the circulation (*Online Supplementary Figure S1*). Importantly, we did not detect clear clinical indications of overt anemia in *Fpr2*$^{-/-}$ mice as determined by complete blood count analysis (*Online Supplementary Figure S2*), though red cell distribution width was trending lower. These findings indicate that deletion of ALX/FPR2 slows the basal rate of erythrocyte turnover, resulting in an aged pool of circulating RBC.

Fpr2$^{-/-}$ mice have decreased splenic markers of red blood cell turnover

Given the observed changes in erythroid turnover in mice lacking ALX/FPR2, we asked whether *Fpr2* deletion had specific impacts on the spleen as this is the primary site of RBC disposal and a critical regulator of erythroid homeostasis. Gross examination and gravimetric analysis (spleen/body weight ratio; *data not shown*) of spleens suggested no differences between WT and *Fpr2*$^{-/-}$ mice. We then performed histological analyses using hematoxylin and eosin-stained tissue sections (Figure 2A) and similarly found that tissue structure was unaltered as quantified by red pulp to white pulp ratio (Figure 2B). Upon closer examination of the tissue, however, we noted an apparent decrease in prevalence of deposits of rich brown staining in the red pulp of *Fpr2*$^{-/-}$ spleens (denoted by arrows in higher magnification images of Figure 2A), which may be indicative of heme or iron deposits. We quantified the abundance of these deposits and found that there were significantly fewer in *Fpr2*$^{-/-}$ spleens (Figure 2C). To further explore whether these deposits reflected areas of RBC turnover, we stained the sections with Prussian blue and found these same regions also had increased amounts of iron (Figure 2D). Moreover, when we quantified the total amount of iron-positive areas in the sections, we determined that the spleens of *Fpr2*$^{-/-}$ mice had significantly less (Figure 2E). As resident macrophages in the red pulp are the cells chiefly responsible for erythrophagocytosis, we performed F4/80 immunostaining of the tissue and found that, as expected, these areas of heme and iron deposits were also highly enriched in macrophages (Figure 2F). To confirm these histological analyses, we performed a colorimetric biochemical assay and found that the total amount of heme in *Fpr2*$^{-/-}$ spleens was decreased (Figure 2G). These data indicate that there is decreased abundance of the prominent intracellular components of RBC in the red pulp of spleens of *Fpr2*$^{-/-}$ mice, suggesting that macrophage-mediated uptake and breakdown of the cells is reduced.

Deletion of *Fpr2* alters the transcriptomes of spleen and splenic macrophages

We next sought to define global alterations in the spleen driven by ALX/FPR2 deletion. To address this, we performed RNA-sequencing analysis of spleens from WT and *Fpr2*$^{-/-}$ mice (Figure 3A). This analysis revealed 61 differentially expressed genes (DEG; 53 downregulated, 8 upregulated) with *Fpr2*, unsurprisingly, being the most significantly affected gene (Figure 3B). Interestingly, *Alox5* and *Alox15* which encode 5-lipoxygenase and 12/15-lipoxygenase, respectively, were also significantly downregulated (Figure 3B). These enzymes are required for the conversion of PUFA substrates into proresolving lipid mediators – including LXA_4, a ligand of ALX/FPR2. To better understand the global changes associated with the identified DEG, we performed gene ontology biological processes (GO:BP) enrichment analysis. Driven largely by *Alox5* and *Alox15*, we found that the Lipoxin Biosynthesis pathway was significantly enriched (Figure 3C). Additional significantly enriched pathways were then clustered based on their biological similarities. Each of these clusters was directly related to innate immune activation and suggested that changes in the myeloid/leukocyte compartment of the tissue were driving the global transcriptomic signature. Macrophages are known sources and targets of SPM, including lipoxins, and are the principal splenic cell type responsible for erythrocyte disposal. Thus, we hypothesized that *Fpr2*$^{-/-}$ deletion acutely targets splenic macrophages.

We isolated F4/80^{+} splenocytes from WT and *Fpr2*$^{-/-}$ mice and performed additional RNA-sequencing analysis (Figure 3D). Here, we found more sweeping changes than in the whole spleens, with 179 total DEG (94 downregulated, 85 upregulated). However, similar to the spleen analysis, we observed that *Fpr2* was the most significantly changed gene and *Alox5* was also downregulated (*Alox15* expression was decreased, albeit not significantly) (Figure 3E). Also similar to the analysis of whole spleen, GO:BP enrichment analysis identified that pathways related to Immune/Inflammatory Response, Defense Response/Response to External Stimuli, and Leukocyte Migration/Chemotaxis were significantly enriched (Figure 3F). Interestingly, however, pathways related to Heme Biosynthesis and Hematopoiesis were also impacted. To understand which significantly changed genes were driving the observed pathway enrichment, we compiled the DEG of each significantly enriched GO pathway and displayed them according to their expression change (Figure 3G). This revealed that the majority of DEG that were

related to the Immune/Inflammatory Response, Leukocyte Migration/Chemotaxis, and Hemopoiesis/Cell Development pathways were downregulated in *Fpr2*$^{-/-}$ mice, while the Defense Response/Response to External Stimuli pathways were represented by DEG that were both upregulated and downregulated. Interestingly, all DEG related to Heme Biosynthesis/Metabolism were upregulated. Considering these data with the findings of the histological examination, this may reflect a compensatory induction of genes related to heme balance in *Fpr2*$^{-/-}$ mice. Taken together, these results indicate that deletion of *Fpr2* induces an altered transcriptomic phenotype in splenic macrophages which may impact the cells' ability to effectively respond to inflammatory stimuli or efficiently perform RBC turnover.

Red pulp macrophages express *Fpr2* and in its absence splenic uptake of stressed red blood cells is impaired

Next, we questioned whether the altered transcriptomes observed in spleens and splenic macrophages of *Fpr2*$^{-/-}$ mice lead to functional impairments that may contribute

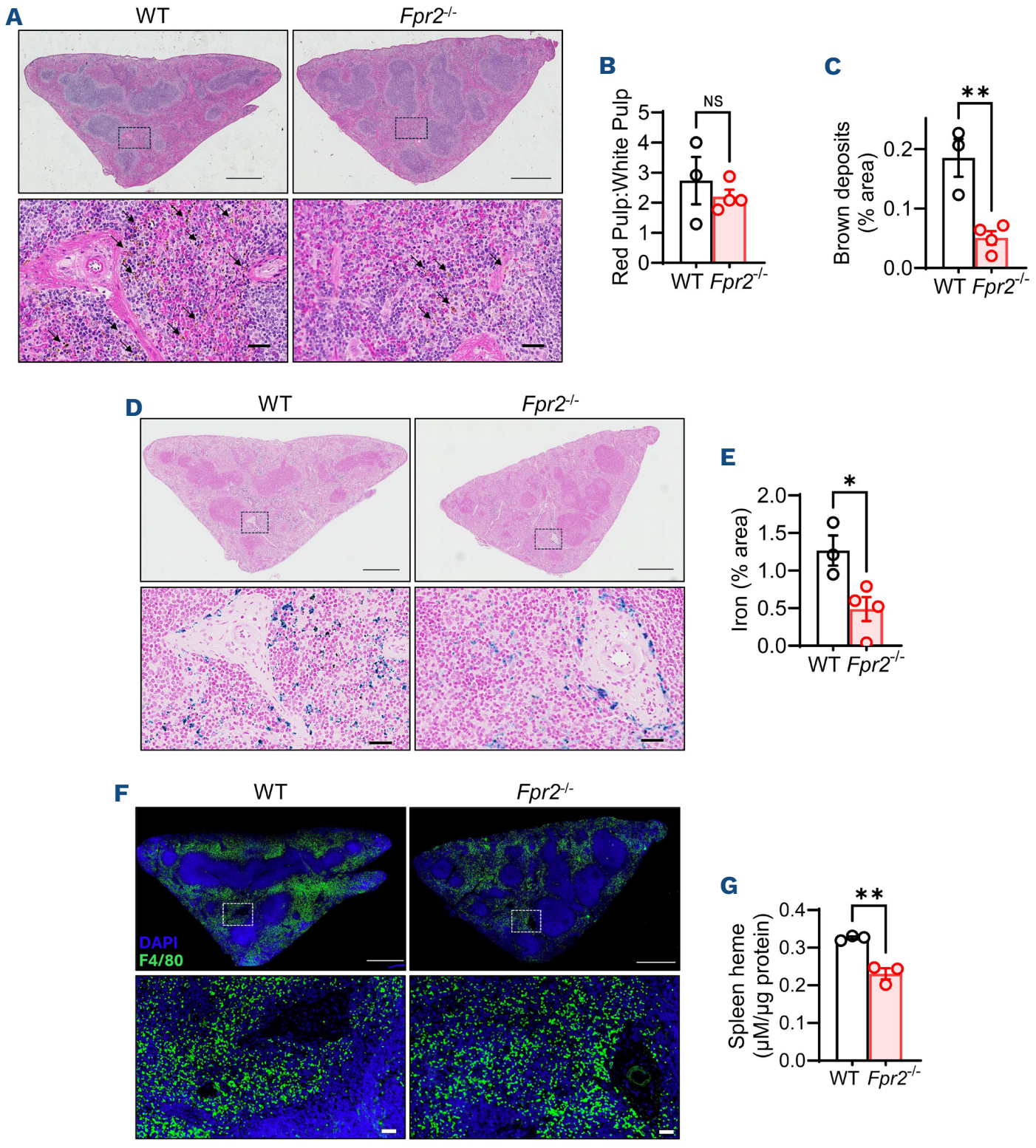

Figure 2. Decreased markers of erythrophagocytosis in spleens of *Fpr2*$^{-/-}$ mice. (A) Representative images of hematoxylin & eosin (H&E)-stained spleen sections. Arrows indicate areas with heme deposits. (B, C) Quantification of the ratio of red pulp to white pulp area (B) and heme deposits (C) as determined from H&E-stained sections. (D, E) Representative images (D) and quantification (E) of iron in Prussian blue-stained spleen sections. (F) Representative images of F4/80-stained spleen sections. (G) Quantification of total spleen heme as determined by colorimetric biochemical assay. (A, D, F) Dashed boxes in images indicate areas of red pulp that are displayed at higher magnification. Scale bars: 500 µm in unmagnified and 30 µm in magnified images. Data are mean ± standard error of mean. N=3-4 per group. *P<0.05, **P<0.01, ***P<0.001, as determined by an unpaired Student t test. WT: wild-type; DAPI: 4-,6-diamidino-2-phenylindole.

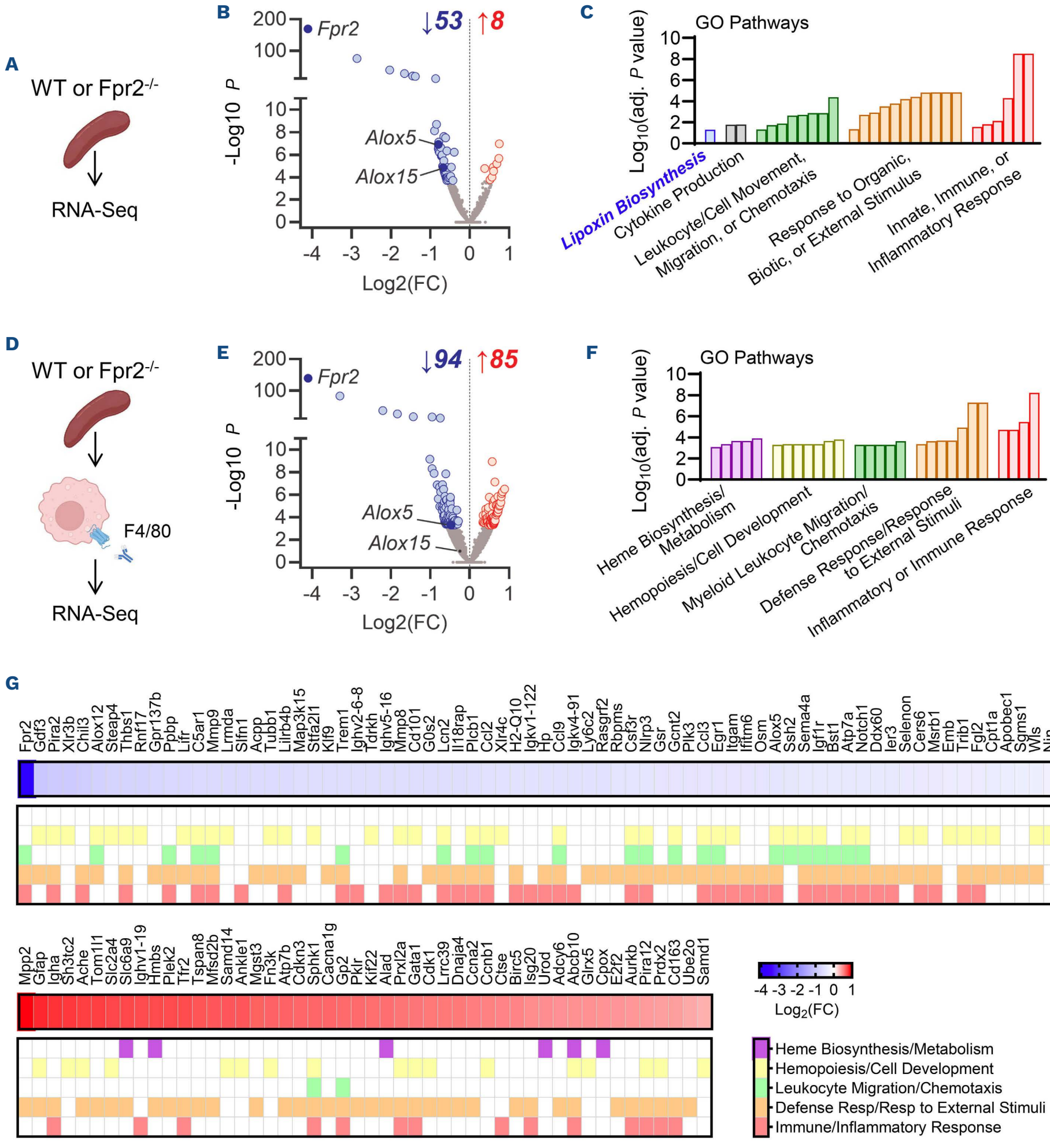

Figure 3. *Fpr2*$^{-/-}$ mice have an altered splenic transcriptome with particular effects on splenic macrophages. (A, D) Schematic of spleens (A) or isolated F4/80^{+} splenocytes (D) from wild-type (WT) and *Fpr2*$^{-/-}$ mice subjected to RNA sequencing. (B, E) Volcano plot analyses of differentially expressed genes (DEG) in spleens (B) or isolated F4/80^{+} splenocytes from *Fpr2*$^{-/-}$ mice compared with those from WT animals. Downregulated genes are shown in blue; upregulated in red. (C, F) Gene ontology (GO): biological process enrichment analyses of DEG displayed with related pathways grouped into functional clusters for spleens (C) and isolated F4/80^{+} splenocytes (F). (G) The change in expression of the component DEG contained in the GO pathways is shown for *Fpr2*$^{-/-}$ F4/80^{+} splenocytes. An accompanying heatmap illustrates the corresponding functional clusters for each DEG. N=3-4 spleens per genotype; N=5 F4/80^{+} splenocyte samples per genotype. RNA-Seq: RNA sequencing; FC: fold-change.

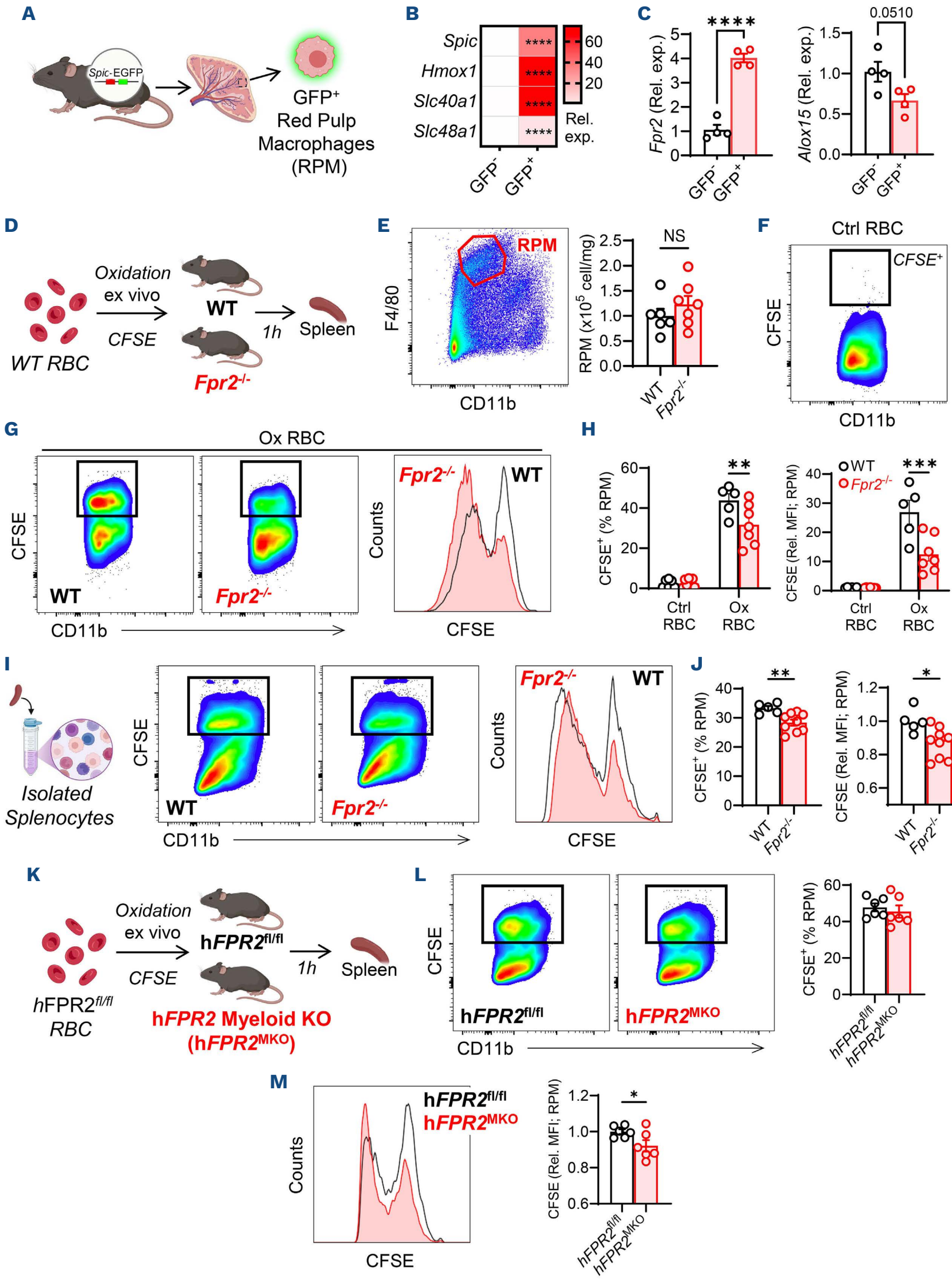

Figure 4. ALX/FPR2 deletion impairs splenic macrophage uptake of damaged red blood cells. (A) Schematic of the *Spic*-enhanced green fluorescent protein (EGFP) reporter mouse. (B, C) Gene expression of flow cytometry-sorted splenocytes from *Spic*-EGFP mice. (D) Schematic of the *in vivo* red blood cell (RBC) uptake assay in wild-type (WT) and *Fpr2*$^{-/-}$ mice. (E) Representative flow cytometry dot plot of splenic red pulp macrophage (RPM) identification and quantification. (F, G) Representative flow cytometry

Continued on following page.

dot plots and overlaid histograms of RPM in WT and *Fpr2*$^{-/-}$ mice 1 h after administration of untreated (Ctrl) or oxidized (Ox) RBC. (H) Quantification of CFSE^{+} RPM and RPM CFSE mean fluorescent imaging (MFI). (I) Primary splenic RPM from WT and *Fpr2*$^{-/-}$ were isolated and incubated *ex vivo* with Ox RBC for 1 h. Representative flow cytometry dot plots and overlaid histograms are shown. (J) Quantification of CFSE^{+} RPM and RPM CFSE MFI. (K) Schematic of *in vivo* RBC uptake assay in humanized *FPR2* floxed mice (h*FPR2*$^{fl/fl}$) and mice with myeloid-specific deletion of human *FPR2* (h*FPR2*^{MKO}). (L) Representative flow cytometry dot plots and quantification of CFSE^{+} RPM and (M) representative flow cytometry overlaid histograms and quantification of RPM CFSE MFI 1 h after administration of Ox RBC. Data are mean ± standard error of mean. (B, C) N=4 per group. (E, H) N=5-7 per group. (J) N=5-9 per group. (K, L) N=6 per group. NS: not statistically significant; **P*<0.05, ***P*<0.01, ****P*<0.001, *****P*<0.0001 as determined by an unpaired Student *t* test (B, C, E, J-L) or two-way analysis of variance (H).

to altered erythrocyte turnover. Recognition and disposal of damaged RBC is a task primarily performed by RPM, a distinct population of splenic resident macrophages. First, we sought to determine whether RPM express *Fpr2*. To definitively identify the RPM population, we used *Spic*-EGFP reporter mice, as *Spic* is the key transcription factor that controls RPM development[26] (Figure 4A). In spleens of these mice, we found that the green fluorescent protein (GFP)$^{+}$ cells were clustered into a distinct population based on expression of CD11b and F4/80 (CD11b^{dim},F4/80^{hi}) while the GFP^{-} cells did not contain this population (*Online Supplementary Figure S3*). To further validate that this population was RPM, we performed flow cytometry-based cell sorting of GFP^{+} and GFP^{-} splenocytes and investigated expression of hallmark RPM genes. As expected, we found that GFP^{+} cells expressed significantly higher levels of *Spic, Hmox1* (heme oxygenase 1), *Slc40a1* (ferroportin), and *Slc48a1* (heme-responsive gene 1) than GFP^{-} cells, confirming their identity as RPM (Figure 4B). We then measured expression of *Fpr2* and found that the receptor was also significantly enriched in RPM compared to non-RPM splenocytes (Figure 4C). Interestingly, we also found that expression of *Alox15* was decreased in RPM which may suggest that non-RPM cells are more responsible for SPM production while RPM are targets of SPM actions.

After validating the identification of RPM by flow cytometry and establishing that RPM express *Fpr2*, we next questioned whether the ability to clear RBC efficiently would be affected in mice lacking ALX/FPR2. To test this, we performed an *in vivo* splenic RBC disposal assay in WT and *Fpr2*$^{-/-}$ mice. RBC from WT donor mice were exposed to an *ex vivo* oxidative insult ($CuSO_4$) prior to labeling with CFSE and delivery (intravenously) to recipient mice (Figure 4D). First, we determined that splenic RPM abundance was not different between WT and *Fpr2*$^{-/-}$ mice (Figure 4E). We then quantified the abundance of CFSE^{+} RPM in spleens of WT and *Fpr2*$^{-/-}$ mice 1 hour after administration of oxidized or control RBC (Figure 4F-H). When unstressed control RBC were delivered, we found that only a small percentage of RPM were CFSE^{+}, indicating a minimal amount of erythrophagocytosis of the exogenous cells. Furthermore, there was no difference in CFSE^{+} RPM in *Fpr2*$^{-/-}$ mice compared with WT after control RBC were administered. However, in mice given oxidized RBC, we detected a sharp increase in the amount of CFSE^{+} RPM, indicating a robust removal of damaged RBC from the circulation. Interestingly, when we compared the extent of oxidized RBC uptake by RPM between genotypes, we noted a striking decrease in both the percentage of RPM that was CFSE^{+} and the RPM CFSE fluorescence in *Fpr2*$^{-/-}$ mice (Figure 4H). To determine whether this defect was due specifically to the lack of ALX/FPR2 signaling on macrophages, we first assessed RBC uptake in isolated primary splenocytes *ex vivo*. Spleens from WT and *Fpr2*$^{-/-}$ mice were harvested and processed into single-cell suspensions and the resulting splenocytes were then incubated with oxidatively damaged, CFSE-labeled RBC (Figure 4I). We found that RPM isolated from *Fpr2*$^{-/-}$ mice displayed decreased uptake of oxidized RBC compared with those from WT mice (Figure 4J), largely recapitulating our *in vivo* observations. Finally, to establish cell specificity *in vivo*, we performed *in vivo* RBC splenic disposal assays using mice with myeloid-specific deletion of *FPR2* (h*FPR2*^{MKO}) (Figure 4K). As described previously,[21] these mice were generated by crossing humanized ALX/FPR2-GFP knockin floxed mice with lysozyme M-Cre-expressing mice. Validation of the loss of ALX/FPR2 expression in peripheral blood leukocytes is shown in *Online Supplementary Figure S4*. Interestingly, we found that while h*FPR2*^{MKO} displayed a similar amount of CFSE^{+} RPM compared with floxed controls (h*FPR2*$^{fl/fl}$), the fluorescence intensity of CFSE within these cells was significantly lower (Figure 4L, M). These results suggest that when *FPR2* is absent from myeloid cells, engulfment of damaged RBC may not be significantly affected but rather the capacity and efficiency of processing ingested RBC cargo is acutely impacted.

Taken together, these data indicate that signaling via ALX/FPR2 specifically on RPM is critical for maintaining a healthy circulating erythroid pool. Given the importance of the receptor in this process, we next questioned whether abundance of ALX/FPR2 ligands changes during erythrophagocytosis.

Heightened erythrophagocytosis stimulates lipoxin A_4 production

To test whether ALX/FPR2 ligand abundance is altered during RBC disposal, we performed targeted liquid chromatography-tandem mass spectrometry lipidomic profiling spanning the arachidonic acid, docosahexaenoic acid, and eicosapentaenoic acid metabolomes. Spleens of WT mice were collected 1 hour after mice had been administered RBC that had either been subjected to the previously described *ex vivo* oxidation of RBC or incubated with a CD47 blocking antibody (CD47 Ab RBC) (Figure 5A, B). Both RBC

treatments led to a clear and marked appearance of $CFSE^+$ cells in the spleen (Figure 5C, D; *Online Supplementary Figure S5*). Lipidomic analysis of spleens following challenge with oxidized RBC demonstrated a clear grouping and separation of samples based on treatment as determined by partial least squares discriminant analysis (PLS-DA), indicating a shift in global lipid mediator profiles (Figure 5E). To determine the specific lipid mediators driving group separation, we performed volcano and variable importance plot analyses (Figure 5F, G). These analyses revealed that nearly all the compounds that were different between treatments were upregulated, spanned each of the parent PUFA metabolomes, and included multiple families of lipid mediators (e.g., lipoxins, resolvins, prostaglandins; representative mass chromatograms of significantly changed lipid mediators are shown in *Online Supplementary Figures S6* and *S7*). Strikingly, however, the most significantly upregulated compound in the analysis was LXA_4. Likewise, when CD47 Ab RBC were delivered we found a similar sample grouping by PLS-DA (Figure 5H) and LXA_4 was among the most upregulated lipid species in the analysis (Figure 5I, J). Absolute quantification of LXA_4 and its parent PUFA (arachidonic acid) confirmed an activation of the lipoxin biosynthetic pathway in both models, albeit with an amplified response after delivery of oxidized RBC compared with CD47 Ab incubation (Figure 5K). Levels of 15-hydroxyeicosatetraenoic acid (15-HETE) were also elevated; however, due to the chromatographic conditions used, we were unable to distinguish between the 15(*R*)- and 15(S)-isomers. While 15(*S*)-HETE is a known intermediate in the enzymatic biosynthesis of LXA_4, we cannot definitively attribute the increase in 15-HETE to the 15(S)-isomer, alone. These results combined with those from *Fpr2*$^{-/-}$ mice demonstrate that splenic LXA_4 production is enhanced during induced erythrophagocytosis and its actions are required for optimal RPM uptake and disposal of damaged RBC.

Lipoxin A_4 increases red blood cell uptake in macrophages *in vitro*

To determine whether LXA_4 directly targets macrophage-mediated uptake of RBC, we employed an *in vitro* approach of differentiating RPM-like cells from isolated murine bone marrow cells (Figure 6A). After stimulation with interleukin-33 and hemin, inducible RPM (iRPM) are enriched in genes characteristic of splenic RPM, mirroring what we measured in the *in vivo*-sorted RPM (Figure 4B), compared to bone marrow-derived macrophages (Figure 6B). Importantly, while iRPM exhibit functional similarities with splenic RPM in their capacity to phagocytose RBC, they do not completely recapitulate the phenotype observed *in vivo*. We determined that iRPM express *Fpr2* similarly to bone marrow-derived macrophages but had decreased expression of *Alox15* (Figure 6C), partially mirroring what we measured in sorted RPM. We then pretreated iRPM with LXA_4 for 15 minutes prior to addition of CFSE-stained RBC and found that this significantly increased their uptake as determined by $CFSE^+$ iRPM and CFSE fluorescence (Figure 6D). These results suggest that LXA_4 stimulates the uptake and removal of RBC via its cognate receptor, ALX/FPR2.

Lipoxin A_4 is critical for efficient red blood cell disposal by splenic red pulp macrophages

Given that LXA_4 abundance was increased in the spleen during heightened RBC uptake and its exogenous administration stimulated increased RBC uptake *in vitro*, we next questioned the impact of disrupting its production on erythrophagocytosis. Using mice with genetic deletion of 12/15-lipoxygenase (*Alox15*$^{-/-}$), a critical LXA_4 biosynthetic enzyme, we first confirmed that LXA_4 abundance in the spleen was indeed decreased (Figure 7A). Next, we subjected the mice to an *in vivo* RBC uptake assay using oxidized RBC (Figure 7B). Similar to what we observed in *Fpr2*$^{-/-}$ mice, we found that mice lacking *Alox15* had no detectable basal difference in RPM-mediated uptake of control RBC but exhibited a significant decrease in erythrophagocytosis of damaged RBC (Figure 7C, D). To test whether exogenous LXA_4 could restore this defect, we administered LXA_4 (intraperitoneally) to WT and *Alox15*$^{-/-}$ mice 15 minutes prior to delivery of oxidized RBC (Figure 7E). Interestingly, we did not observe an LXA_4-induced enhancement of RPM uptake in WT mice, but in those lacking *Alox15*$^{-/-}$ there was an increase, restoring levels of uptake to that of WT mice (Figure 7F, G). These results suggest that LXA_4 is sufficient to enhance RPM-mediated clearance of RBC.

Discussion

In this study, we establish an integral role for ALX/FPR2 signaling in maintaining erythroid homeostasis. In mice lacking ALX/FPR2, we found elevated levels of aged RBC in the circulation, indicating a decreased rate of basal turnover. Histological analyses of spleens from *Fpr2*$^{-/-}$ mice showed decreased abundance of heme and iron deposits in red pulp, further suggesting decreased RBC turnover, while transcriptomics revealed an altered splenic macrophage phenotype, driven in part by changes in heme metabolism. Functionally, we found that during on-demand erythrophagocytosis splenic production of LXA_4, a key proresolving ligand of ALX/FPR2, was increased in WT mice. However, in mice lacking ALX/FPR2 or the biosynthetic enzyme critical for LXA_4 production (i.e., 12/15-LOX), erythrophagocytosis was impaired. Critically, myeloid-specific deletion of *FPR2* also impaired efficient splenic erythrophagocytosis. Finally, when administered exogenous LXA_4, the deficient erythrophagocytosis of *Alox15*$^{-/-}$ mice was restored. Together, these results indicate that in response to RBC stress splenic LXA_4 production is enhanced, activating ALX/FPR2 on RPM to promote erythrophagocytosis and removal of dysfunctional erythrocytes from the circulation to maintain hematologic homeostasis. The findings presented here offer new insights into the

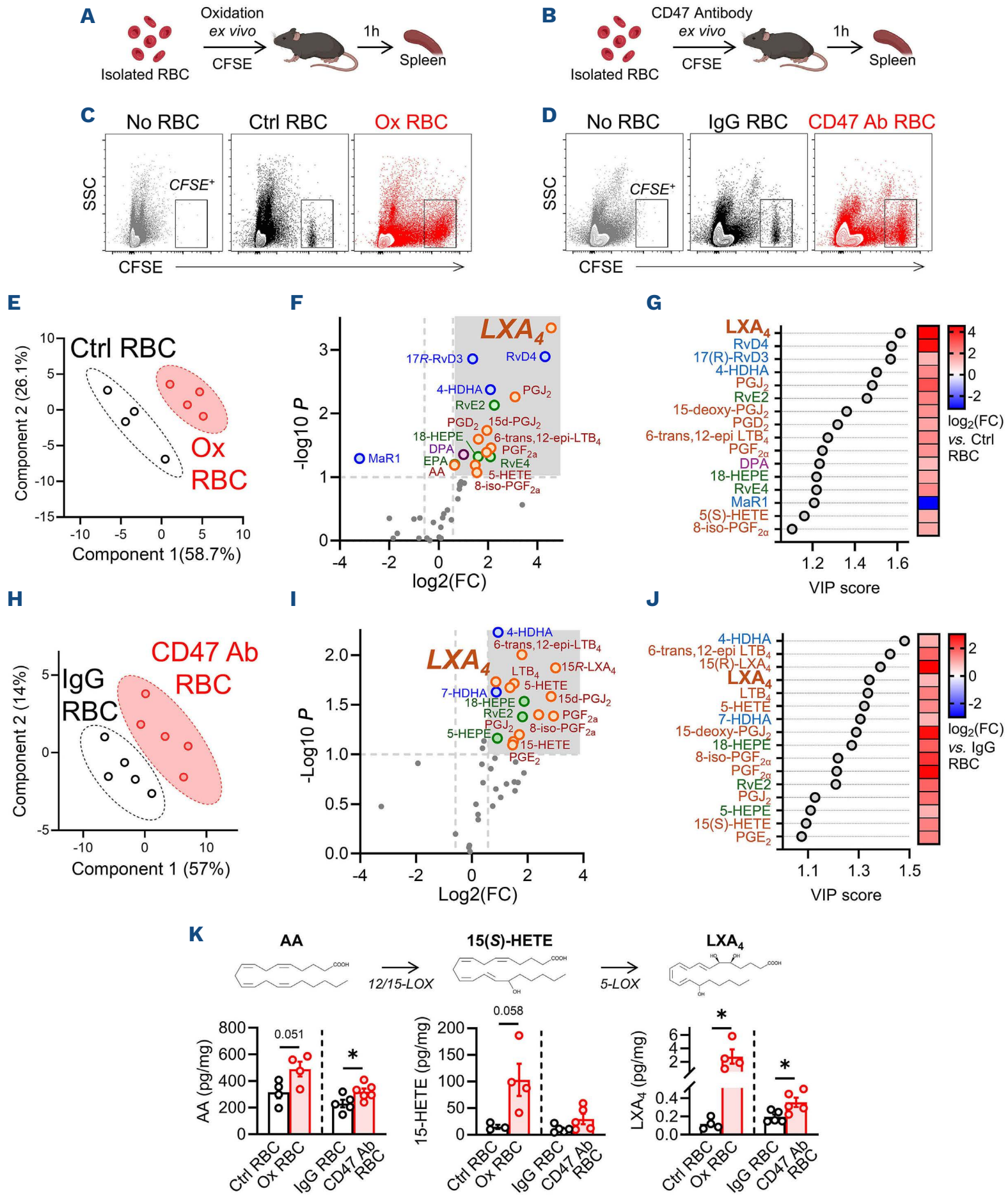

Figure 5. Lipoxin A_4 is increased during splenic uptake of damaged red blood cells. (A, B) Schematic of *in vivo* uptake assays in which red blood cells (RBC) were oxidized (A) or incubated with CD47 blocking antibody or IgG control antibody (B) *ex vivo* prior to administration (via retro-orbital injection). (C-K) Spleens were removed 1 h later and subjected to flow cytometric (C, D) or targeted liquid chromatography tandem mass spectrometry lipidomic analyses (E-K). (C, D) Representative flow cytometric dot plots showing $CFSE^+$ cells in spleen. (E, H) Plots of partial least squares discriminant analysis two-dimensional scores showing clustering of samples based on their global lipidomic profiles. (F, G, I, J) Volcano plots (F, I) and variable importance plots (G, J) displaying significantly changed lipid mediators colored according to their parent fatty acid (orange – arachidonic acid; blue – docosahexaenoic acid; green – eicosapentaenoic acid; purple – docosapentaenoic acid). (K) Absolute abundance of selected arachidonic acid-derived lipid mediators. Data are mean ± standard error of mean. N=4 per group (control *vs*. oxidized RBC); N=5 per group (RBC incubated with IgG *vs*. CD47 blocking antibody). *P<0.05 as determined by an unpaired Student t test *versus* appropriate control group. SSC: side scatter; Ctrol: control; Ox: oxidized; CFSE: carboxyfluorescein succinimidyl ester; IgG RBC: RBC incubated with immunoglobulin G; CD47 Ab RBC: RBC incubated with CD47 blocking antibody; FC: fold change; VIP: variable importance in projection; AA: arachidonic acid; 15(S)-HETE: 15-hydroxyeicosatetraenoic acid; LXA_4: lipoxin A_4.

mechanisms of local proresolving signaling pathways significantly impacting systemic immune processes. By acting locally on macrophages in the spleen LXA_4-ALX/FPR2 signaling is necessary to preserve an optimal population of circulating erythrocytes while it is also sufficient to overcome acute erythroid stress. The ability to influence the RBC pool is critical as small variations in the fitness of erythrocytes can have profound physiological and immunological effects.[27,28] As RBC age or are stressed they undergo a variety of alterations including modifications in metabolism, morphology, and membrane structure which result in functional decline characterized by decreased ability to facilitate gas exchange and an increased risk of aggregation.[29-31] Additionally, recent reports have suggested that RBC also have a direct immunomodulatory impact via their ability to bind and deliver inflammatory agonists such as cytokines and nucleic acids, stimulating innate immune responses.[32,33] Thus, preserving a healthy pool of circulating RBC is important in mediating the risks of infection, anemia, and thrombosis, and is critical in the body's response to malaria and sickle cell disease.

Recently it was demonstrated that targeting the ALX/FPR2 receptor with proresolving ligands during a sickle cell crisis may be a beneficial treatment strategy as mice exhibited ameliorated cerebral thrombosis[34] and vaso-occlusive pathologies.[22] While the importance of ALX/FPR2 in the development and progression of cardiovascular diseases, such as atherosclerosis,[35] aortic aneurysm,[36,37] heart failure,[38-40] and infection-induced cardiac dysfunction[41,42] has been well-documented, its role in hematologic pathologies remains comparatively unexplored.

Results of our study complement and extend previous work that has established a role for proresolving lipid mediators in erythrocyte uptake and disposal[22,23,43-46] by

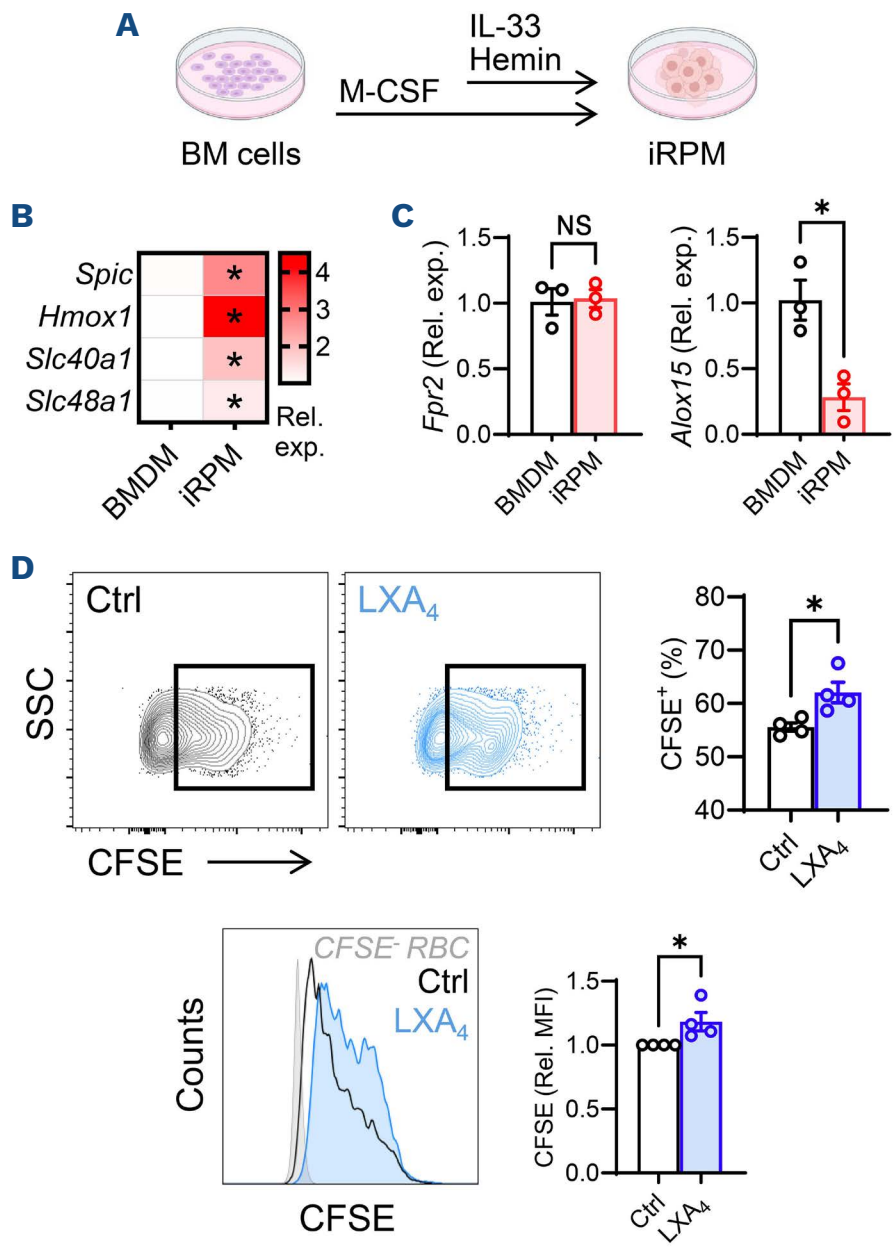

Figure 6. Lipoxin A_4 stimulates macrophage uptake of red blood cells. (A) Schematic of *in vitro* generation of induced red pulp macrophages (iRPM) from bone marrow cells using macrophage colony-stimulating factor, interleukin-33, and hemin. (B, C) Gene expression in iRPM and bone marrow-derived macrophages. (D) Representative flow cytometry dot plots, overlaid histograms, and quantification of iRPM following stimulation for 15 minutes with LXA_4 prior to addition of CFSE-stained red blood cells. Data are mean ± standard error of mean. (B, C) N=3 or (D) N=4 independent experiments including at least three technical replicates per experiment. **P*<0.05 as determined by an unpaired Student *t* test; NS: not statistically significant; BM: bone marrow; M-CSF: macrophage colony-stimulating factor; IL-33: interleukin-33; BMDM; bone marrow-derived macrophages; Rel. exp.: relative expression; SSC: side scatter; Ctrl: control; CFSE: carboxyfluorescein succinimidyl ester; LXA_4: lipoxin A_4; Rel. MFI: relative mean fluorescent intensity.

demonstrating the myeloid dependence of ALX/FPR2 signaling on the process. These previous reports found that the abundance of SPM, including ALX/FPR2 ligands, is decreased in spleens of mice with sickle cell disease and demonstrate the ability of D- and E-series resolvins, as well as the recently described cysteinyl-resolvins, to promote macrophage uptake of senescent RBC *in vivo* and *in vitro*. However, the impact of LXA_4, specifically, has not been described nor has the essential role of ALX/FPR2. In our models of induced erythrophagocytosis we found that the abundance of SPM species in spleen was broadly increased, with LXA_4 being the most significantly induced mediator. In addition to LXA_4, we found that levels of RvD4, 17*R*-RvD3, Maresin 1, RvE2, and RvE4 were increased after challenge with oxidized RBC. RvE4 has previously been shown to be biosynthesized during co-incubation of human RBC and

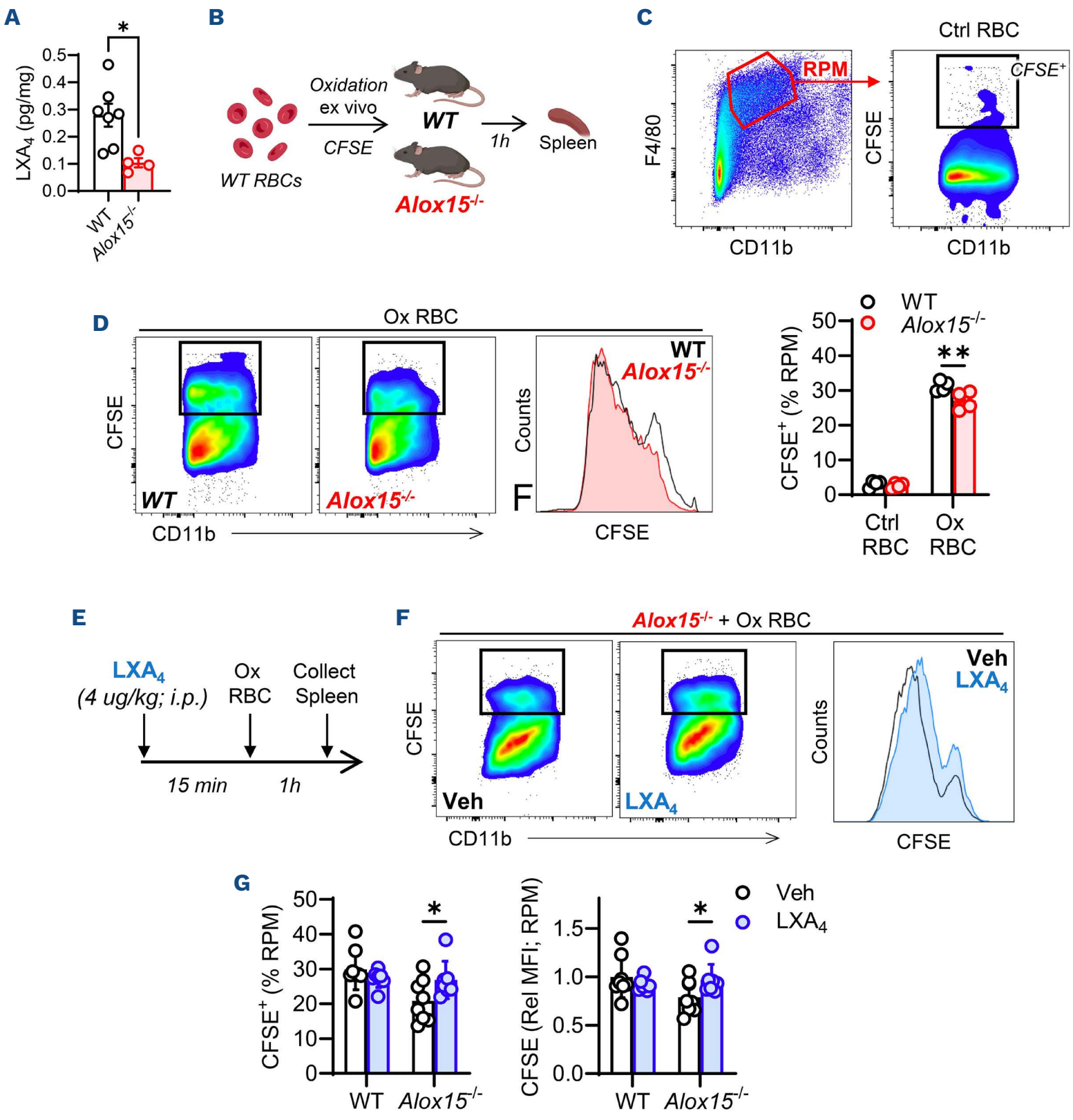

Figure 7. Lipoxin A_4 is sufficient to rescue defective erythrophagocytosis. (A) Lipoxin A_4 (LXA_4) abundance in spleens of wild-type (WT) and 12/15-lipoxygenase deficient (*Alox15*$^{-/-}$) mice. N= 4-7 per group. (B) Schematic of the *in vivo* red blood cell (RBC) uptake assay in WT and *Alox15*$^{-/-}$ mice. (C, D) Representative flow cytometry dot plots and quantification of carboxyfluorescein succinimidyl ester (CFSE)-positive splenic red pulp macrophages (RPM) in WT and *Alox15*$^{-/-}$ mice 1 hour after administration of untreated (Ctrl) or oxidized (Ox) RBC. N=4 per group (D). (E) Schematic of the *in vivo* uptake assay in which WT and *Alox15*$^{-/-}$ mice received exogenous LXA_4 or vehicle (Veh) 15 minutes prior to Ox RBC administration. (F) Representative flow cytometry dot plots and overlaid histograms of RPM from *Alox15*$^{-/-}$ mice following vehicle (Veh) or LXA_4 treatment and Ox RBC administration. (G) Quantification of $CSFE^+$ RPM (%) and RPM CFSE mean fluorescent intensity. N=7–8 per group. Data are mean ± standard error of mean. **P*<0.05, ***P*<0.01 as determined by an unpaired Student *t* test (A) or two-way analysis of variance (D, G).

macrophages, and stimulation with RvE4 potently enhanced erythrophagocytosis in human macrophages.[44] We also detected an increased abundance of 17*R*-RvD3. This is notable as the related mediator and ALX/FPR2 ligand, 17*R*-RvD1, was previously found to be decreased in spleens of sickle cell mice and its administration was sufficient to enhance splenic RBC disposal[22] and to improve cardiomyopathy in humanized sickle cell mice.[47] Although we did not identify 17*R*-RvD1, both mediators are derived from the aspirin- or cyclooxygenase-2-dependent conversion of docosahexaenoic acid but differ in their subsequent biosynthetic routes and epoxide intermediates. While it is not clear that 17*R*-RvD3 can bind and activate ALX/FPR2, its epimer, RvD3, is a known ligand of the receptor.[48,49]

Importantly, much of the previous work referenced above was conducted in a humanized mouse model of sickle cell anemia. It has been demonstrated that while these mice share important phenotypic similarities as humans with sickle cell disease, they also display marked changes in splenic morphology, particularly related to the red pulp.[50] Conversely, the current study was performed in healthy mice with no overt splenic morbidity. Thus, the results presented here demonstrate the critical importance of this signaling pathway to basal splenic erythrocyte processing and maintenance of hemodynamic homeostasis.

The current study provides new mechanistic insight into the role of ALX/FPR2 in erythroid homeostasis. For the first time, we have demonstrated a macrophage-intrinsic defect in erythrophagocytosis in the absence of ALX/FPR2 signaling, using both isolated primary RPM and mice with myeloid-specific deletion of the receptor. Interestingly, comparing the impact of global and myeloid-specific knockout of *Fpr2* revealed a divergence in erythrophagocytic function. While RPM from myeloid-deficient mice could recognize and engulf damaged RBC similarly to floxed controls, their reduced fluorescence intensity indicated a lower RBC load per cell. This suggests that without ALX/FPR2, RPM may become functionally satiated more quickly, with impaired capacity for simultaneous degradation of multiple RBC. Additionally, RNA sequencing from *Fpr2*$^{-/-}$ isolated splenic macrophages revealed significant changes in heme metabolism pathways, pointing to a potential defect in processing of RBC-derived heme. Although the mechanism for this reduced RBC processing remains unclear, it may involve intermediary metabolism, which is increasingly recognized as essential for macrophages to degrade multiple apoptotic cells.[51-53] Indeed, we have previously shown that ALX/FPR2 activation promotes mitochondrial metabolism and efferocytosis via AMPK-dependent signaling.[54-56] Additionally, given that RBC digestion releases significant quantities of reactive species (e.g., heme, iron), ALX/FPR2-mediated suppression of reactive oxygen species production may help RPM to adapt during high-demand erythrophagocytic conditions. This aligns with recent reports demonstrating that ALX/FPR2 activation protects against macrophage ferroptosis.[36,57] While our findings establish a functional role for the LXA_4–ALX/FPR2 signaling axis in enhancing splenic erythrophagocytosis, further studies are needed to elucidate the underlying mechanisms more fully.

Overall, our findings reveal new functions of the LXA_4-ALX/FPR2 signaling axis and contribute to a growing body of literature assigning importance to lipid mediators in the uptake and disposal of aged or damaged erythrocytes. These findings offer an additional physiological mechanism that may bolster the capability of ALX/FPR2 activation to combat systemic unresolved inflammation and inform the development of new therapeutic approaches to target the pathway during transfusion-related immunomodulation or acute hemolytic crises.

Disclosures

No conflicts of interest to disclose.

Contributions

HA, HHD, J-JZ and RS performed experiments, analyzed data and wrote the manuscript. JLH designed experiments, supervised research and wrote the manuscript. BES conceived and planned the project, supervised research, analyzed data and wrote the manuscript. BES is the guarantor of this work and, as such, had full access to the data and takes responsibility for the integrity of the data and the accuracy of the data analysis.

Funding

Support for this work was provided by the NIH (R01ES034389; R01GM127495; P30GM127607). Computational resources and bioinformatics pipelines were provided by the KY INBRE Bioinformatics Core with funding from the National Institute of General Medical Sciences, NIH (P20GM103436). Its contents are solely the responsibility of the authors and do not necessarily represent the official views of the NIH.

Data-sharing statement

RNA-sequencing data have been deposited in the NCBI GEO database with the accession numbers GSE292685 and GSE292686.

References

1. Klei TR, Meinderts SM, van den Berg TK, et al. From the cradle to the grave: the role of macrophages in erythropoiesis and erythrophagocytosis. Front Immunol. 2017;8:73.
2. Neri S, Swinkels DW, Matlung HL, et al. Novel concepts in red blood cell clearance. Curr Opin Hematol. 2021;28(6):438-444.
3. Slusarczyk P, Mleczko-Sanecka K. The multiple facets of iron

recycling. Genes (Basel). 2021;12(9):1364.
4. Muckenthaler MU, Rivella S, Hentze MW, et al. A red carpet for iron metabolism. Cell. 2017;168(3):344-361.
5. Hod EA, Zhang N, Sokol SA, et al. Transfusion of red blood cells after prolonged storage produces harmful effects that are mediated by iron and inflammation. Blood. 2010;115(21):4284-4292.
6. Youssef LA, Rebbaa A, Pampou S, et al. Increased erythrophagocytosis induces ferroptosis in red pulp macrophages in a mouse model of transfusion. Blood. 2018;131(23):2581-2593.
7. Woodruff AW, Ansdell VE, Pettitt LE. Cause of anaemia in malaria. Lancet. 1979;1(8125):1055-1057.
8. Michel M, Crickx E, Fattizzo B, et al. Autoimmune haemolytic anaemias. Nat Rev Dis Primers. 2024;10(1):82.
9. Costea N. The differential diagnosis of hemolytic anemias. Med Clin North Am. 1973;57(2):289-302.
10. Serhan CN. Pro-resolving lipid mediators are leads for resolution physiology. Nature. 2014;510(7503):92-101.
11. Serhan CN, Levy BD. Resolvins in inflammation: emergence of the pro-resolving superfamily of mediators. J Clin Invest. 2018;128(7):2657-2669.
12. Decker C, Sadhu S, Fredman G. Pro-resolving ligands orchestrate phagocytosis. Front Immunol. 2021;12:660865.
13. Chiang N, Arita M, Serhan CN. Anti-inflammatory circuitry: lipoxin, aspirin-triggered lipoxins and their receptor ALX. Prostaglandins Leukot Essent Fatty Acids. 2005;73(3-4):163-177.
14. Maderna P, Cottell DC, Toivonen T, et al. FPR2/ALX receptor expression and internalization are critical for lipoxin A4 and annexin-derived peptide-stimulated phagocytosis. FASEB J. 2010;24(11):4240-4249.
15. Fiore S, Maddox JF, Perez HD, et al. Identification of a human cDNA encoding a functional high affinity lipoxin A4 receptor. J Exp Med. 1994;180(1):253-260.
16. Krishnamoorthy S, Recchiuti A, Chiang N, et al. Resolvin D1 binds human phagocytes with evidence for proresolving receptors. Proc Natl Acad Sci U S A. 2010;107(4):1660-1665.
17. Sansbury BE, Spite M. Resolution of acute inflammation and the role of resolvins in immunity, thrombosis, and vascular biology. Circ Res. 2016;119(1):113-130.
18. Fredman G, Serhan CN. Specialized pro-resolving mediators in vascular inflammation and atherosclerotic cardiovascular disease. Nat Rev Cardiol. 2024;21(11):808-823.
19. Giannakis N, Sansbury BE, Patsalos A, et al. Dynamic changes to lipid mediators support transitions among macrophage subtypes during muscle regeneration. Nat Immunol. 2019;20(5):626-636.
20. Hellmann J, Sansbury BE, Wong B, et al. Biosynthesis of D-series resolvins in skin provides insights into their role in tissue repair. J Invest Dermatol. 2018;138(9):2051-2060.
21. Sansbury BE, Li X, Wong B, et al. Myeloid ALX/FPR2 regulates vascularization following tissue injury. Proc Natl Acad Sci U S A. 2020;117(25):14354-14364.
22. Matte A, Recchiuti A, Federti E, et al. Resolution of sickle cell disease-associated inflammation and tissue damage with 17R-resolvin D1. Blood. 2019;133(3):252-265.
23. Norris PC, Libreros S, Serhan CN. Resolution metabolomes activated by hypoxic environment. Sci Adv. 2019;5(10):eaax4895.
24. Saxena RK, Bhardwaj N, Sachar S, et al. A double in vivo biotinylation technique for objective assessment of aging and clearance of mouse erythrocytes in blood circulation. Transfus Med Hemother. 2012;39(5):335-341.
25. Oldenborg PA, Zheleznyak A, Fang YF, et al. Role of CD47 as a marker of self on red blood cells. Science. 2000;288(5473):2051-2054.
26. Kohyama M, Ise W, Edelson BT, et al. Role for Spi-C in the development of red pulp macrophages and splenic iron homeostasis. Nature. 2009;457(7227):318-321.
27. Dobkin J, Mangalmurti NS. Immunomodulatory roles of red blood cells. Curr Opin Hematol. 2022;29(6):306-309.
28. Niu C, Zhang J. Immunoregulation role of the erythroid cells. Front Immunol. 2024;15:1466669.
29. Bosch FH, Werre JM, Schipper L, et al. Determinants of red blood cell deformability in relation to cell age. Eur J Haematol. 1994;52(1):35-41.
30. Mohanty JG, Nagababu E, Rifkind JM. Red blood cell oxidative stress impairs oxygen delivery and induces red blood cell aging. Front Physiol. 2014;5:84.
31. Weisel JW, Litvinov RI. Red blood cells: the forgotten player in hemostasis and thrombosis. J Thromb Haemost. 2019;17(2):271-282.
32. Karsten E, Breen E, Herbert BR. Red blood cells are dynamic reservoirs of cytokines. Sci Rep. 2018;8(1):3101.
33. Lam LKM, Murphy S, Kokkinaki D, et al. DNA binding to TLR9 expressed by red blood cells promotes innate immune activation and anemia. Sci Transl Med. 2021;13(616):eabj1008.
34. Ansari J, Senchenkova EY, Vital SA, et al. Targeting the AnxA1/Fpr2/ALX pathway regulates neutrophil function, promoting thromboinflammation resolution in sickle cell disease. Blood. 2021;137(11):1538-1549.
35. Drechsler M, de Jong R, Rossaint J, et al. Annexin A1 counteracts chemokine-induced arterial myeloid cell recruitment. Circ Res. 2015;116(5):827-835.
36. Filiberto AC, Ladd Z, Leroy V, et al. Resolution of inflammation via RvD1/FPR2 signaling mitigates Nox2 activation and ferroptosis of macrophages in experimental abdominal aortic aneurysms. FASEB J. 2022;36(11):e22579.
37. Petri MH, Thul S, Andonova T, et al. Resolution of inflammation through the lipoxin and ALX/FPR2 receptor pathway protects against abdominal aortic aneurysms. JACC Basic Transl Sci. 2018;3(6):719-727.
38. Garcia RA, Lupisella JA, Ito BR, et al. Selective FPR2 agonism promotes a proresolution macrophage phenotype and improves cardiac structure-function post myocardial infarction. JACC Basic Transl Sci. 2021;6(8):676-689.
39. Kain V, Ingle KA, Colas RA, et al. Resolvin D1 activates the inflammation resolving response at splenic and ventricular site following myocardial infarction leading to improved ventricular function. J Mol Cell Cardiol. 2015;84:24-35.
40. Kain V, Liu F, Kozlovskaya V, et al. Resolution agonist 15-epi-lipoxin A(4) programs early activation of resolving phase in post-myocardial infarction healing. Sci Rep. 2017;7(1):9999.
41. Chen J, Austin-Williams S, O'Riordan CE, et al. Formyl peptide receptor type 2 deficiency in myeloid cells amplifies sepsis-induced cardiac dysfunction. J Innate Immun. 2023;15(1):548-561.
42. das Dores Pereira R, Rabelo RAN, Leite PG, et al. Role of formyl peptide receptor 2 (FPR2) in modulating immune response and heart inflammation in an experimental model of acute and chronic Chagas disease. Cell Immunol. 2021;369:104427.
43. Nshimiyimana R, Libreros S, Simard M, et al. Stereochemistry and functions of the new cysteinyl-resolvin, 4S,5R-RCTR1, in efferocytosis and erythrophagocytosis of human senescent erythrocytes. Am J Hematol. 2023;98(7):1000-1016.
44. Reinertsen AF, Libreros S, Nshimiyimana R, et al. Metabolization of resolvin E4 by omega-oxidation in human neutrophils: synthesis and biological evaluation of 20-hydroxy-resolvin E4 (20-OH-RvE4). ACS Pharmacol Transl Sci. 2023;6(12):1898-1908.

45. Libreros S, Shay AE, Nshimiyimana R, et al. A new E-series resolvin: RvE4 stereochemistry and function in efferocytosis of inflammation-resolution. Front Immunol. 2020;11:631319.
46. Simard M, Nshimiyimana R, Chiang N, et al. A potent proresolving mediator 17R-resolvin D2 from human macrophages, monocytes, and saliva. Sci Adv. 2024;10(47):eadq4785.
47. Federti E, Mattoscio D, Recchiuti A, et al. 17(R)-Resolvin D1 protects against sickle cell-related inflammatory cardiomyopathy in humanized mice. Blood. 2025;145(17):1915-1928.
48. Arnardottir HH, Dalli J, Norling LV, et al. Resolvin D3 is dysregulated in arthritis and reduces arthritic inflammation. J Immunol. 2016;197(6):2362-2368.
49. Dalli J, Winkler JW, Colas RA, et al. Resolvin D3 and aspirin-triggered resolvin D3 are potent immunoresolvents. Chem Biol. 2013;20(2):188-201.
50. Kamimura S, Smith M, Vogel S, et al. Mouse models of sickle cell disease: imperfect and yet very informative. Blood Cells Mol Dis. 2024;104:102776.
51. Schilperoort M, Ngai D, Sukka SR, et al. The role of efferocytosis-fueled macrophage metabolism in the resolution of inflammation. Immunol Rev. 2023;319(1):65-80.
52. Yurdagul A Jr, Subramanian M, Wang X, et al. Macrophage metabolism of apoptotic cell-derived arginine promotes continual efferocytosis and resolution of injury. Cell Metab. 2020;31(3):518-533.e10.
53. Zhang S, Weinberg S, DeBerge M, et al. Efferocytosis fuels requirements of fatty acid oxidation and the electron transport chain to polarize macrophages for tissue repair. Cell Metab. 2019;29(2):443-456.e5.
54. Calderin EP, Zheng JJ, Boyd NL, et al. Exercise-induced specialized proresolving mediators stimulate AMPK phosphorylation to promote mitochondrial respiration in macrophages. Mol Metab. 2022;66:101637.
55. Hosseini Z, Marinello M, Decker C, et al. Resolvin D1 enhances necroptotic cell clearance through promoting macrophage fatty acid oxidation and oxidative phosphorylation. Arterioscler Thromb Vasc Biol. 2021;41(3):1062-1075.
56. Pena Calderin E, Zheng JJ, Boyd NL, et al. Exercise-stimulated resolvin biosynthesis in the adipose tissue is abrogated by high-fat diet-induced adrenergic deficiency. Arterioscler Thromb Vasc Biol. 2025;45(7):1090-1110.
57. Li X, Xu H, Liu K, et al. LXA4 alleviates inflammation and ferroptosis in cigarette smoke induced chronic obstructive pulmonary disease via the ALX/FPR2 receptor. Int Immunopharmacol. 2025;151:114322.